IX. GASEOUS ELECTRONICS*

Academic and Research Staff

Prof. G. Bekefi
Prof. S. C. Brown
Prof. J. C. Ingraham
Prof. B. L. Wright
Dr. W. M. Manheimer
J. J. McCarthy
W. J. Mulligan

Graduate Students

W. B. Davis
G. A. Garosi

A. SOME EFFECTS OF FLOW ON A MEDIUM PRESSURE ARGON DISCHARGE

This report presents further work done on the Argon gas flow discharge system reported on previously.[1,2]

1. Plasma Spectrum

In accordance with the assumption of frozen flow, the plasma density wave-number spectrum can be obtained from a frequency analysis of the current drawn by a negatively biased electrostatic probe immersed in the plasma.[2] The density spectra obtained are in good agreement with those obtained by V. L. Granatstein et al.[3,4] The spectra show an inertial (Kolmogoroff) range where the spectrum function, $E_{nl}(K)$, has a $K^{-5/3}$ dependence on K. This range is not developed for the flow with Reynolds number, Re, of 2400. The spectra also show a viscous range which demonstrates a K^{-7} dependence. The slight deviation from K^{-7} shown in Fig. IX-1 may be attributed to noise in the plasma. (The spectra functions were plotted against frequency in Fig. IX-1 so that all three could be plotted on the same graph without undue crowding. For frozen flow we have $K = 2\pi f/\overline{U}$, where $\overline{U}$ is the mean flow velocity at the electrostatic probe, and thus frequency and wave-number plots are analogous.) The spectra also showed a $K^{-13/3}$ region that has been interpreted by V. L. Granatstein[3] as being due to the enhanced diffusion of plasma particles when compared with molecular diffusion for the gas atoms. We shall return to this point later.

2. Density Fluctuations

As was reported previously[2] the density fluctuations were measured with a radially movable probe. The radial profile of density fluctuations and of average density reported there seemed to indicate, as suggested by V. L. Granatstein,[4] a relationship between the intensity of the fluctuations and the gradient of the average density. It was

*This work was supported by the Joint Services Electronics Programs (U. S. Army, U. S. Navy, and U. S. Air Force) under Contract DA 28-043-AMC-02536(E).

further suggested by H. M. Schulz[5] that, because of the tendency of the Argon discharge at these pressures (p ≈ 20 Torr) to constrict and thus not "fill" the entire tube, the

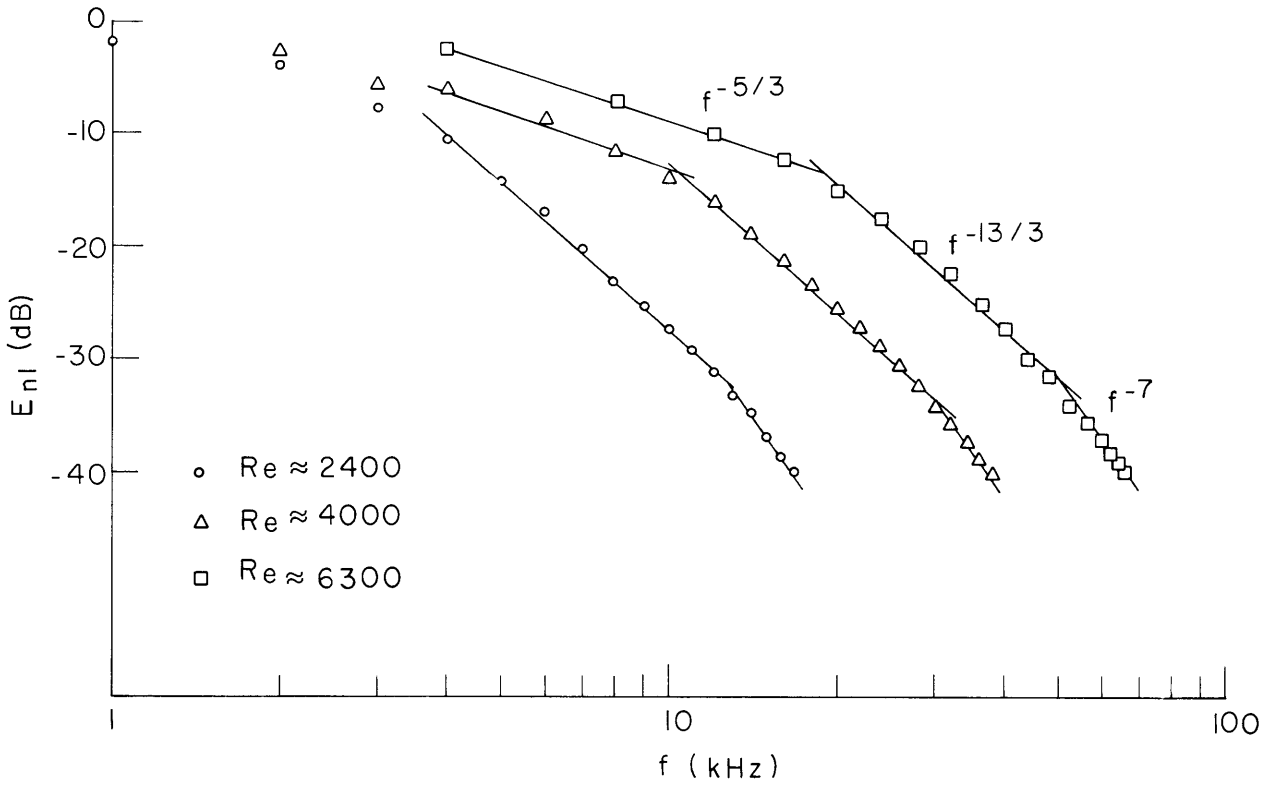

Fig. IX-1. Spectra of density fluctuations.

fluctuations recorded by a probe fixed in space may be resulting from a gross movement of the column. Such an interpretation was also suggested by V. L. Granatstein[3] in order to explain some radial density correlation results obtained by him.

In order to test this interpretation the data were analyzed, under the assumption of the following model. If we assume an infinitely long, axially symmetric cylindrical discharge, the density can then be represented by a two-dimensional function, $n(\vec{r}) = n_o f(\vec{r})$ (see Fig. IX-2 for the coordinate system used). We now permit the discharge column to move so that the probability of the center of the column being at position R is given by P(R). Thus we have for the average density and for the mean of the square[5]

$$\langle n(r) \rangle = n_o \int f(p)\, P(R)\, d^3R \tag{1}$$

$$\langle n^2(r) \rangle = n_o^2 \int f^2(\rho)\, P(R)\, d^3R, \tag{2}$$

where P(R) is defined so that

$$\int P(R)\, d^3R = 1 \tag{3}$$

and $\rho^2 = r^2 + R^2 - 2r\, R \cos\theta$.

It was found that for low flows, that is, flow values low enough so that the discharge

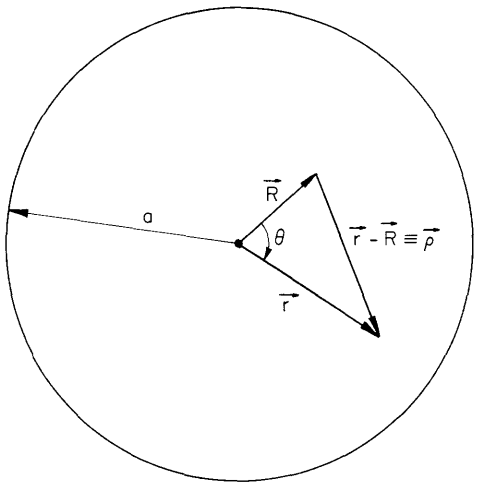

Fig. IX-2. Coordinate system.

was not noticeably affected, the density profile could be represented by a Gaussian,

$$f(\rho) = \exp\left(-\frac{\rho^2}{\langle\rho^2\rangle}\right). \tag{4}$$

It was further assumed that P(R) is a Gaussian

$$P(R) = \frac{1}{\pi\langle R^2\rangle} \exp\left(-\frac{R^2}{\langle R^2\rangle}\right). \tag{5}$$

Substituting Eqs. 4 and 5 in Eqs. 1 and 2 yields, after integrating,

$$\langle n(r)\rangle = \frac{n_o}{\langle\rho^2\rangle + \langle R^2\rangle} \exp\left[-\frac{r^2}{\langle\rho^2\rangle + \langle R^2\rangle}\right] \tag{6}$$

$$\langle n^2(r)\rangle = \frac{n_o^2}{\langle\rho^2\rangle + 2\langle R^2\rangle} \exp\left[-\frac{2r^2}{\langle\rho^2\rangle + 2\langle R^2\rangle}\right] \tag{7}$$

from which we obtain

$$\frac{\langle n(r)\rangle^2}{\langle n^2(r)\rangle} = \frac{1 + 2\xi}{1 + 2\xi + \xi^2} \exp\left[-\frac{2r^2}{\rho^2} \frac{\xi}{(1+\xi)(1+2\xi)}\right], \tag{8}$$

where

$$\xi = \frac{\langle R^2\rangle}{\langle \rho^2\rangle}.$$

Equation 8 tells us that if our assumptions are correct a plot of $\log_e [\langle n^2(r)\rangle / \langle n(r)\rangle^2]$ against r^2 should yield a straight line. From the slope and the intercept of such a plot it is possible to obtain values for $\langle R^2\rangle$ and $\langle \rho^2\rangle$. It is expected that the assumptions, and thus Eq. 8, may break down near the tube walls, since the integrals were performed under the assumption that the tube wall was essentially at infinity. As an approximate idea of the limits of this assumption we can say that the assumptions will be suspect for

$$e^{-a^2/\langle Y^2\rangle} \gtrsim 0.1 \Longrightarrow \frac{\langle Y^2\rangle}{a^2} \gtrsim 0.5, \tag{9}$$

where a is the radius of the tube, and $\langle Y^2\rangle$ is the larger of $\langle R^2\rangle$ or $\langle \rho^2\rangle$.

If the density is represented by

$$n(t) = \bar{n} + n'(t), \tag{10}$$

where the bar indicates a time average and $\overline{n'(t)} = 0$, then it follows that

$$\overline{n^2(t)} = \bar{n}^2 + \overline{(n'(t))^2}. \tag{11}$$

Now the averaging indicated in Eqs. 6-8 can be interpreted as a time average over the large scale disturbances in the plasma. Furthermore, the density power spectra shown in Fig. IX-1 indicate that the bulk of the fluctuation intensity is located in these large-scale (low-frequency) fluctuations. Thus an instrument that time averages over the entire frequency spectrum of the density fluctuations (such as an unfiltered rms voltmeter) will be performing, essentially, the averaging process associated with Eqs. 6-8. Thus we may write Eq. 11 as

$$\langle n^2\rangle = \langle n\rangle^2 + \langle (n')^2\rangle \tag{12}$$

or

$$\frac{\langle n(r)\rangle^2}{\langle n^2(r)\rangle} = \left[1 + \frac{\langle (n'(r))^2\rangle}{\langle n(r)\rangle^2}\right]^{-1}. \tag{13}$$

The values for $\langle(n'(r))^2\rangle$ were obtained with a Hewlett-Packard Model 3400A rms voltmeter which has a frequency response from 10 Hz to 10MHz.

In Fig. IX-3 we have some representative plots of the experimental data. Although the plotted data are for pressure, p, of 25 Torr and a discharge current, I_d, of 1.8 A, data for other currents (0.5 A-1.8 A) and pressures (15-35 Torr) gave similar results. As expected, the deviation from a straight line for $(r/a)^2 > 0.5$ was quite marked in some cases, but the agreement for $(r/a)^2 \lesssim 0.5$ ($r/a \lesssim 0.7$) is extremely encouraging.

In Fig. IX-4 we have the values of $\langle R^2\rangle/a^2$ and $\langle\rho^2\rangle/a^2$ derived from the data plotted against the flow parameter, Q_o. As a self-consistency check we note that Eq. 6 says that the mean density should have a Gaussian profile with a width given by

$$\frac{\langle x^2\rangle}{a^2} = \frac{\langle R^2\rangle + \langle\rho^2\rangle}{a^2}. \tag{14}$$

Plots of $(\langle R^2\rangle + \langle\rho^2\rangle)/a^2$ and the measured values, $\langle x^2\rangle/a^2$, are given in Fig. IX-4 and are in fairly good agreement.

In Fig. IX-5 we give some representative plots to show the degree of accuracy of the assumptions, since any strong deviation of the mean density profile from a Gaussian would signify a breakdown of one or all of the assumptions. An implicit assumption is that the plasma column does not change size, no matter what the value of R. This is obviously invalid when the column gets sufficiently close to the wall, approximately for $a - R \lesssim \sqrt{\langle\rho^2\rangle}$, and will probably be the first assumption to become invalid.

The plots in Fig. IX-5 and similar data for other flow values, pressures, and discharge currents indicate that the assumptions are consistently good for $(r^2/a)^2 \lesssim 0.5$ for low flows, but become poorer for the higher flow where the column motion becomes significant, $\langle R^2\rangle/a^2 \gtrsim 0.5$. Our conclusion is that for bulk processes the interpretation given by Eqs. 6-8 is valid but that effects occurring near the wall such as wall losses for the plasma require a more sophisticated approach.

By examining Fig. IX-4 we see that the plasma column remains constricted even under the influence of large flows. The strong variation of $\langle\rho^2\rangle/a^2$ with flow for $Q_o \lesssim 300$ cm^3/sec is believed to be due mainly to variations in gas temperature resulting from the cooling effect of the incoming gas. The initial increase of $\langle\rho^2\rangle/a^2$ corresponds with an initial increase in the gas temperature. The interpretation of the active discharge response to flow is still under consideration and will be reported on later.

Returning to Fig. IX-4, it is observed that there exists disturbances in the flow (that is, finite values of $\langle R^2\rangle$), for flows below the "critical" Reynolds number for pipe turbulence, Re $\approx$ 1900. These low-flow disturbances result for instabilities in the basically laminar flow.[6,7] The transition from stable laminar flow to fully developed turbulence in a pipe or channel involves a sequence of increasingly complex laminar

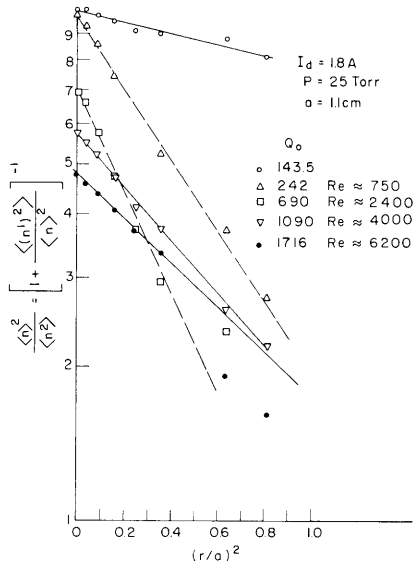

Fig. IX-3. Experimental results.

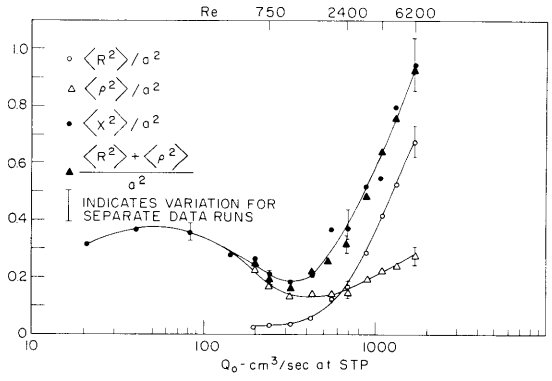

Fig. IX-4. Density profile parameters.

flow regimes that may support local turbulent motion at sufficiently large distances from the input region.[8, 9] The study of liquid flow in a pipe done by E. R. Lindgren[9] showed

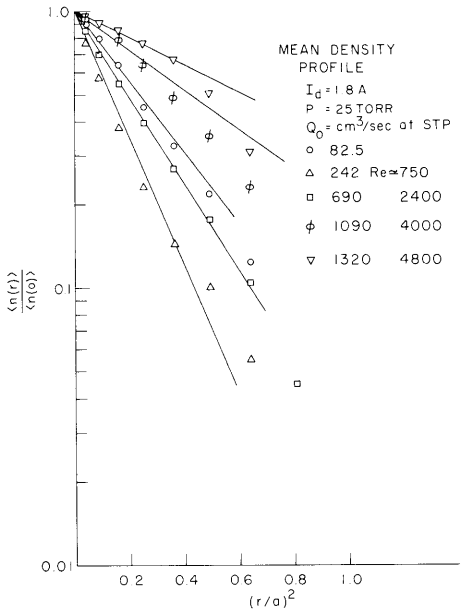

Fig. IX-5. Plots to show degree of accuracy of the assumptions.

that the level of fluid disturbance, especially in the entrance region, was strongly dependent on the presence of disturbances in the flow channel. Since the tube used in my experiment had a length of only 30 tube diameters, it is felt that the flow behavior will be a function of the level of disturbances present at the entrance.

3. Spatial Afterglow Experiment

In order to obtain a direct measure of the effect of turbulent gas flow on the plasma loss mechanism it was decided to study the plasma in the region downstream of the active discharge (Fig. IX-6). It was decided to use a DC discharge to produce the plasma and electrostatic probes for diagnostics, since such an approach was readily adaptable to the existing experimental setup.

There are certain disadvantages evident in this arrangement. First, the presence of the electrode will produce a disturbance that may be difficult to compensate for. Second, the use of electrostatic probes will require knowledge of the electron

temperature and, for lower densities, will require knowledge of the sheath thickness, which is small, and thus negligible, for conditions of the active discharge.[1] Third, the use of more than one probe introduces problems of calibration and dissimilar probe perturbations of the plasma. For these and other reasons, the study on this tube is still in progress.

Electron temperature measurements were made using the single probe technique as discussed previously.[1] These results are given in Fig. IX-7. The electron temperatures, V_e, for later times were at first thought to be erroneously large. A crude calculation for the cooling of electrons via elastic collisions with gas atoms, which can be obtained from

$$\tau \approx 1/g\nu_c, \tag{15}$$

where τ is the electron temperature decay time constant, $g = 2m/M$ is the fractional energy transfer per collision, and ν_c is the electron-neutral collision frequency, shows that for Argon gas at 20 Torr pressure and $V_e \approx 1$ eV the electrons should lose a significant fraction of their energy in times of the order of 6 μsec. It was thus decided to check the electron temperature by an alternative method.

As we have mentioned, the spectrum of the density fluctuations showed a region in which the decay of eddies in K (frequency) space was due to the ambipolar diffusion of plasma particles. As reported by V. L. Granatstein[3] this inertial-diffusive regime should have a range given by

$$\frac{f_\nu}{f_D} = \frac{K_\nu}{K_D} = \left(\frac{D}{\nu}\right)^{3/4}, \tag{16}$$

where D is the ambipolar diffusion coefficient, and ν is the kinematic viscosity. Substituting values for the Argon discharge at $p \approx 20$ Torr and $I_d \approx 1.8$ A, we obtain

$$\frac{f_\nu}{f_D} \approx [.3(1+T_e/T)]^{3/4}, \tag{17}$$

when T_e and T are the electron and gas temperatures, respectively. It was assumed in writing Eq. 17 that the ions are at the same temperature as the gas. Some representative spectra are plotted in Fig. IX-8.

On account of the uncertainty associated with the coefficient $(.3)^{3/4}$ appearing in Eq. 17, the electron temperature was obtained by comparing the range of the inertial-diffusive region for the various times with the corresponding range for spectra measured in the active discharge. By letting the subscript zero refer to the active discharge conditions, one obtains from Eq. 17

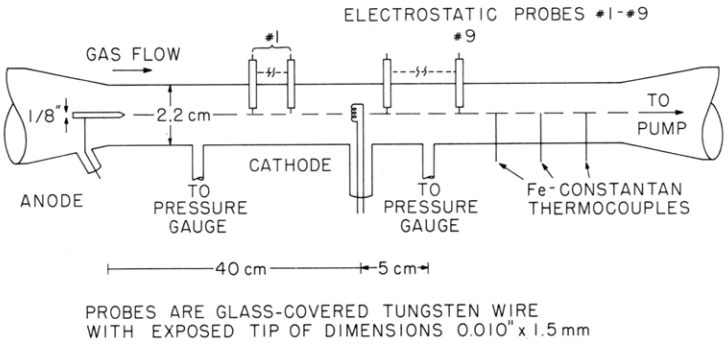

Fig. IX-6. Tube for spatial afterglow experiment.

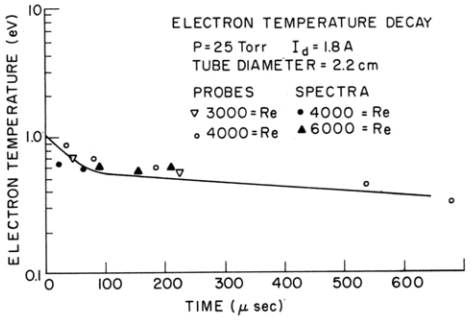

Fig. IX-7. Results of measurements with single-probe technique.

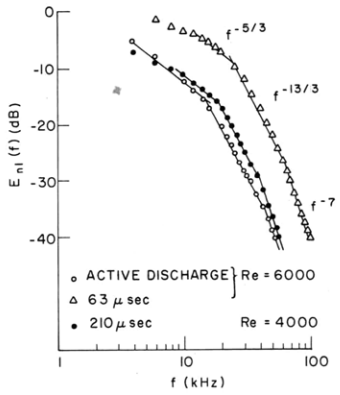

Fig. IX-8. Frequency spectrum in the afterglow.

$$\frac{T_e}{(T_e)_o} \approx \frac{T}{(T)_o} \frac{[f_\nu/f_d]^{4/3}}{[f_\nu/f_d]_o^{4/3}}, \tag{18}$$

where it was assumed that $T_e \gg T$. The temperatures thus obtained are also plotted in Fig. IX-7.

Although the agreement between the two at small times is somewhat less than overwhelming, the spectra results, which are not as subject to the problem of probe surface cleanliness as are the single-probe curve results, do seem to support the probe curve results. The reason for such a high electron temperature for times greater than 100 μsec is still unknown.

G. A. Garosi

References

1. G. Garosi, Quarterly Progress Report No. 86, Research Laboratory of Electronics, Massachusetts Institute of Technology, July 15, 1967, pp. 129-134.
2. G. Garosi, Quarterly Progress Report No. 89, Research Laboratory of Electronics, Massachusetts Institute of Technology, April 15, 1968, pp. 99-109.
3. V. L. Granatstein et al., Phys. Rev. Letters 16, 504 (1966).
4. V. L. Granatstein, Phys. Fluids 10, 1236 (1967).
5. H. M. Schulz III, Private communication, 1967.
6. J. O. Hinze, Turbulence (McGraw-Hill Book Company, Inc., New York, (1959), pp. 68-69.
7. C. C. Lin, The Theory of Hydrodynamic Stability (Cambridge University Press, London, 1966).
8. V. V. Struminskii, Phys. Fluids 10, S95 (1967).
9. E. R. Lindgren, Arkiv För Fysik 7, 293 (1953); Arkiv För Fysik 15, 97 (1959); Arvik För Fysik 15, 503 (1959).